arXiv:1407.1456v1 [hep-ph] 6 Jul 2014

Probing the R-parity violating supersymmetric effects in the exclusive $c \to d/s\ell\nu_\ell$ decays

Ru-Min Wang*, Jie Zhu, Jin-Huan Sheng, Mo-Lin Liu, Yuan-Guo Xu

College of Physics and Electronic Engineering, Xinyang Normal University, Xinyang, Henan 464000, China

July 8, 2014

Abstract

A lot of branching ratios of the exclusive $c \to d/s\ell\nu_\ell$ ($\ell = e, \mu$) decays have been quite accurately measured by CLEO-c, BELLE, BABAR, BES(I,II,III), ALEPH and MARKIII collaborations. We probe the R-parity violating supersymmetric effects in the exclusive $c \to d/s\ell\nu_\ell$ decays. From the latest experimental measurements, we obtain new upper limits on the relevant R-parity violating coupling parameters within the decays, and many upper limits are obtained for the first time. Using the constrained new parameter spaces, we predict the R-parity violating effects on the observables, which have not been measured or have not been well measured yet. We find that the R-parity violating effects due to slepton exchange could be large on the branching ratios of $D_{d/s} \to e\nu_e$ decays and the normalized forward-backward asymmetries of $D_{u/d} \to \pi/K\ell\nu_\ell$ as well as $D_s \to K\ell\nu_\ell$ decays, and all branching ratios of the relevant semileptonic D decays are sensitive to squark exchange couplings. Our results in this work could be used to probe new physics effects in the leptonic decays as well as the semileptonic decays, and will correlate with searches for direct supersymmetric signals at LHC and BESIII.

PACS Numbers: 13.20.Fc, 12.60.Jv, 11.30.Er, 12.15.Mm

*E-mail:ruminwang@gmail.com

1 Introduction

The $c \to d/s\ell\nu_\ell$ transitions have played a central role for the most precise measurements of CKM matrix elements V_{cd} and V_{cs} for a long time. These rare charmed decays also have received a lot of attention, since they are very promising for investigating the standard model (SM) and searching for new physics (NP) beyond it. The 26 charmed decays, $D_d \to \ell\nu_\ell$, $D_u \to \pi\ell\nu_\ell$, $D_d \to \pi\ell\nu_\ell$, $D_s \to K\ell\nu_\ell$, $D_u \to \rho\ell\nu_\ell$, $D_d \to \rho\ell\nu_\ell$, $D_s \to K^*\ell\nu_\ell$, $D_s \to \ell\nu_\ell$, $D_u \to K\ell\nu_\ell$, $D_d \to K\ell\nu_\ell$, $D_u \to K^*\ell\nu_\ell$, $D_d \to K^*\ell\nu_\ell$ and $D_s \to \phi\ell\nu_\ell$, are dominated by $c \to d/s\ell\nu_\ell$ transitions. Many collaborations, such as BSEIII [1–4], CLEO-c [5–12] and BELLE [13, 14], BABAR [15, 16], BESII [17], BES [18–21], ALEPH [22] and MARK-III [23], have studied the exclusive $c \to d/s\ell\nu_\ell$ decays, and a lot of branching ratios have been quite accurately measured by them. Present experimental measurements are in good agreement with the SM predictions, and they give us an opportunity to disprove NP or find bounds over NP models beyond the SM.

The exclusive $c \to d/s\ell\nu_\ell$ decays have been studied extensively in the SM and its various extensions (see for instance Refs. [24–33]). In the present study, we will analyze these decays in supersymmetry (SUSY) without R-parity. We will obtain eight new upper limits on the relevant supersynmmetric coupling parameters that satisfy all of the experimental data from the relevant charmed decays. Using the constrained new parameter spaces, we will predict the R-parity violating (RPV) effects on the branching ratios, the differential branching ratios and the normalized forward-backward asymmetries of charged leptons. Our results imply that the constrained RPV couplings due to slepton exchange have great effects on $\mathcal{B}(D_{d/s} \to e\nu_e)$, and they could obviously enhance the allowed ranges of $\mathcal{A}_{FB}(D \to P\ell\nu_\ell)$. Nevertheless, the RPV contributions due to squark exchange couplings could enhance the predictions of all semileptonic branching ratios, which are very sensitive to the relevent RPV coupling products.

This paper is schemed as follows: In section 2, we introduce the theoretical frame of the exclusive $c \to d/s\ell\nu_\ell$ decays in SUSY without R-parity. In section 3, we deal with the numerical results. We display the constrained parameter spaces which satisfy all the available experimental data, and then we use the constrained parameter spaces to predict the RPV effects on other quantities, which have not been measured or have not been well measured yet. Section 4 contains our summary and conclusion.

2 The exclusive $c \to d/s\ell\nu_\ell$ decays in SUSY without R-parity

In the SM, the $c \to d/s\ell\nu_\ell$ processes are mediated by a virtual W boson exchange, and the relevant four fermion effective Hamiltonian is

$$\mathcal{H}_{eff}^{SM}(\bar{c} \to \bar{d}_k \ell_m^+ \nu_{\ell_n}) = \frac{G_F}{\sqrt{2}} V_{cd_k}^* (\bar{d}_k \gamma_\mu (1-\gamma_5) c)(\bar{\nu}_{\ell_n} \gamma^\mu (1-\gamma_5) \ell_m). \tag{1}$$

In the most general superpotential of SUSY, the RPV superpotential is given by [34]

$$\mathcal{W}_{\not R_p} = \mu_i \hat{L}_i \hat{H}_u + \frac{1}{2}\lambda_{[ij]k} \hat{L}_i \hat{L}_j \hat{E}_k^c + \lambda'_{ijk} \hat{L}_i \hat{Q}_j \hat{D}_k^c + \frac{1}{2}\lambda''_{i[jk]} \hat{U}_i^c \hat{D}_j^c \hat{D}_k^c, \tag{2}$$

where $\hat{L}$ and $\hat{Q}$ are the SU(2)-doublet lepton and quark superfields, $\hat{E}^c$, $\hat{U}^c$ and $\hat{D}^c$ are the singlet superfields, while i, j and k are generation indices and c denotes a charge conjugate field. From Eq. (2), one can get the relevant R-parity breaking part of the Lagrangian of $\bar{c} \to \bar{d}_j \ell_m^+ \nu_{\ell_n}$ [35, 36]

$$\begin{aligned} \mathcal{L}_{eff}^{\not R_p}(\bar{c} \to \bar{d}_k \ell_m^+ \nu_{\ell_n}) &= -\sum_{i,j,k} \tilde{\lambda}'_{ijk} \left[\tilde{\ell}_{iL} \bar{d}_{kR} u_{jL} + \tilde{d}_{kR}^* \bar{\ell}_{iR}^c u_{jL} \right] \\ &\quad + \sum_{i,j,k} \lambda'_{ijk} \left[\tilde{d}_{kR}^* \bar{\nu}_{\ell_i R}^c d_{jL} \right] + \sum_{i,j,k} \lambda_{ijk} \left[\tilde{\ell}_{jL} \bar{\ell}_{kR} \nu_{\ell_i L} \right], \end{aligned} \tag{3}$$

with $\tilde{\lambda}_{irk} \equiv \sum_n V_{rn}^* \lambda_{ink}$, and V_{rn} is the SM CKM matrix element. Noted that (s)down-down-(s)neutrino vertices have the weak eigenbasis couplings λ', while charged (s)lepton-(s)down-(s)up vertices have the up quark mass eigenbasis couplings $\tilde{\lambda}'$. Very often in the literature (see e.g. [37–41]), one neglects the difference between λ' and $\tilde{\lambda}'$, based on the fact that diagonal elements of the CKM matrix dominate over nondiagonal ones.

In terms of Eq.(3), we can obtain the relevant four fermion effective Hamiltonian for the $\bar{c} \to \bar{d}_j \ell_m^+ \nu_{\ell_n}$ processes with RPV couplings due to the squark and slepton exchange

$$\begin{aligned} \mathcal{H}_{eff}^{\not R_p}(\bar{c} \to \bar{d}_k \ell_m^+ \nu_{\ell_n}) &= -\sum_i \frac{\lambda'^*_{nki} \tilde{\lambda}'_{m2i}}{8 m^2_{\tilde{d}_{iR}}} (\bar{d}_k \gamma_\mu (1-\gamma_5) c)(\bar{\nu}_{\ell_n} \gamma^\mu (1-\gamma_5) \ell_m) \\ &\quad + \sum_i \frac{\lambda^*_{inm} \tilde{\lambda}'_{i2k}}{4 m^2_{\tilde{\ell}_{iL}}} (\bar{d}_k (1-\gamma_5) c)(\bar{\nu}_{\ell_n} (1+\gamma_5) \ell_m). \end{aligned} \tag{4}$$

And the corresponding RPV feynman diagrams for the $\bar{c} \to \bar{d}_k \ell_m^+ \nu_{\ell_n}$ processes are displayed in Fig. 1.

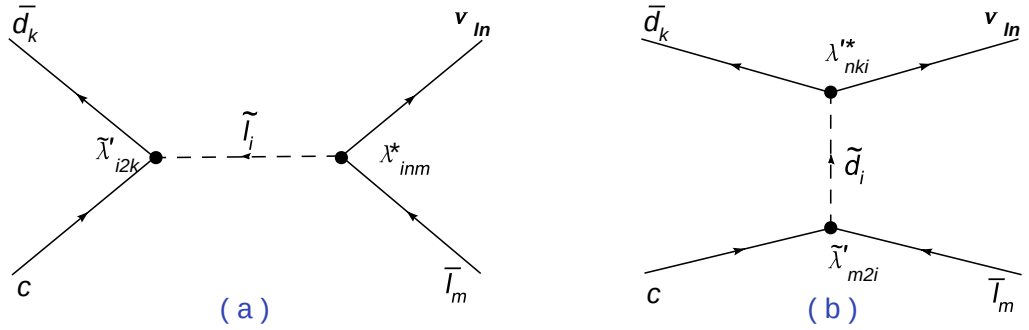

Figure 1: The RPV contributions to the exclusive $\bar{c} \to \bar{d}_k \ell_m^+ \nu_{\ell_n}$ decays due to slepton and squark exchange.

Then we can obtain the total effective Hamiltonian for the $\bar{c} \to \bar{d}_k \ell_m^+ \nu_{\ell_n}$ in the RPV SUSY

$$\mathcal{H}_{eff}(\bar{c} \to \bar{d}_k \ell_m^+ \nu_{\ell_n}) = \mathcal{H}_{eff}^{SM}(\bar{c} \to \bar{d}_k \ell_m^+ \nu_{\ell_n}) + \mathcal{H}_{eff}^{\not{R}_p}(\bar{c} \to \bar{d}_k \ell_m^+ \nu_{\ell_n}). \tag{5}$$

Based on the effective Hamiltonian in Eq. (5), we will give the expressions of physical quantities for the RPV SUSY later in detail. In the following expressions and numerical analysis, we will keep the masses of the charged leptons, but ignore all neutrino masses.

2.1 $D_{d/s} \to \ell \nu_\ell$ decays

Purely leptonic decays are the simplest and the cleanest decay modes of the pseudoscalar charged D^+ meson, and the decay amplitude of $D_{d_k}^+ \to \ell^+ \nu_\ell$ can be obtained in the terms of Eq.(5)

$$\begin{aligned}
\mathcal{M}^{\not{R}_p}(D_{d_k}^+ \to \ell_m^+ \nu_{\ell_n}) &= < \ell_m^+ \nu_{\ell_n} | \mathcal{H}_{eff}(\bar{c} \to \bar{d}_k \ell_m^+ \nu_{\ell_n}) | D_{d_k}^+ > \\
&= \left[\frac{G_F}{\sqrt{2}} V_{cd_k}^* - \sum_i \frac{\lambda'^*_{nki} \tilde{\lambda}'_{m2i}}{8 m^2_{\tilde{d}_{iR}}} \right] < 0 | \bar{d}_k \gamma_\mu (1-\gamma_5) c | D_{d_k}^+ > (\bar{\nu}_{\ell_n} \gamma^\mu (1-\gamma_5) \ell_m) \\
&\quad + \sum_i \frac{\lambda^*_{inm} \tilde{\lambda}'_{i2k}}{4 m^2_{\tilde{\ell}_{iL}}} < 0 | \bar{d}_k (1-\gamma_5) c | D_{d_k}^+ > (\bar{\nu}_{\ell_n} (1+\gamma_5) \ell_m).
\end{aligned} \tag{6}$$

After using the definitions of D meson decay constant [42]

$$< 0 | \bar{d}_k \gamma_\mu \gamma_5 c | D^+(p) >= i f_D p_\mu, \tag{7}$$

and

$$< 0 | \bar{d}_k \gamma_5 c | D^+(p) >= -i f_D \mu_{D_q} \quad \text{with} \quad \mu_{D_{d_k}} \equiv \frac{m^2_{D_{d_k}}}{\bar{m}_c + \bar{m}_{d_k}}, \tag{8}$$

we get the branching ratio for $D^+_{d/s} \to \ell^+\nu_\ell$

$$\begin{aligned}\mathcal{B}^{R_p}(D^+_{d_k} \to \ell^+_m \nu_{\ell_n}) &= \left|\frac{G_F}{\sqrt{2}}V^*_{cd_k} - \sum_i \frac{\lambda'^*_{nki}\tilde{\lambda}'_{m2i}}{8m^2_{\tilde{d}_{iR}}} + \sum_i \frac{\lambda^*_{inm}\tilde{\lambda}'_{i2k}}{4m^2_{\tilde{\ell}_{iL}}}\frac{\mu_{D_{d_k}}}{m_{\ell_m}}\right|^2 \\ &\times \frac{\tau_{D_{d_k}}}{4\pi} f^2_{D_{d_k}} m_{D_{d_k}} m^2_{\ell_m}\left[1 - \frac{m^2_{\ell_m}}{m^2_{D_{d_k}}}\right]. \end{aligned} \tag{9}$$

2.2 $D \to P\ell\nu_\ell$ $(P = \pi, K)$ decays

In the terms of Eq.(5), $D \to P\ell^+\nu_\ell$ decay amplitude can be written as

$$\begin{aligned}\mathcal{M}^{R_p}(D \to P\ell^+_m\nu_{\ell_n}) &= \left\langle P\ell^+_m\nu_{\ell_n}|\mathcal{H}_{eff}(\bar{c} \to \bar{d}_k\ell^+_m\nu_{\ell_n})|D\right\rangle \\ &= \left[\frac{G_F}{\sqrt{2}}V^*_{cd_k} - \sum_i \frac{\lambda'^*_{nki}\tilde{\lambda}'_{m2i}}{8m^2_{\tilde{d}_{iR}}}\right]\left\langle P|\bar{d}_k\gamma_\mu(1-\gamma_5)c|D\right\rangle(\bar{\nu}_{\ell_n}\gamma^\mu(1-\gamma_5)\ell_m) \\ &+ \sum_i \frac{\lambda^*_{inm}\tilde{\lambda}'_{i2k}}{4m^2_{\tilde{\ell}_{iL}}}\left\langle P|\bar{d}_k(1-\gamma_5)c|D\right\rangle(\bar{\nu}_{l_n}(1+\gamma_5)\bar{\ell}_m). \end{aligned} \tag{10}$$

Using the $D \to P$ transition form factors [43]

$$c_P\left\langle P(p)\left|\bar{d}_k\gamma_\mu c\right|D(p_D)\right\rangle = f^P_+(s)(p+p_D)_\mu + \left[f^P_0(s) - f^P_+(s)\right]\frac{m^2_D - m^2_P}{s}q_\mu, \tag{11}$$

$$c_P\left\langle P(p)\left|\bar{d}_k c\right|D(p_D)\right\rangle = f^P_0(s)\frac{m^2_D - m^2_P}{\bar{m}_c - \bar{m}_{d_k}}, \tag{12}$$

with the factor c_P accounts for the flavor content of particles ($c_P = \sqrt{2}$ for π^0, and $c_P = 1$ for π^-, K^0, K^-) and $s = q^2$ ($q = p_D - p$), the differential branching ratio for $D \to P\ell^+_m\nu_{\ell_n}$ is

$$\frac{d\mathcal{B}^{R_p}(D \to P\ell^+_m\nu_{\ell_n})}{dsdcos\theta} = \frac{\tau_D\sqrt{\lambda_P}}{2^7\pi^3 m^3_D c^2_P}\left(1 - \frac{m^2_{\ell_m}}{s}\right)^2\left[N^P_0 + N^P_1 cos\theta + N^P_2 cos^2\theta\right], \tag{13}$$

with

$$\begin{aligned}N^P_0 &= \left|\frac{G_F}{\sqrt{2}}V^*_{cd_k} - \sum_i \frac{\lambda'^*_{nki}\tilde{\lambda}'_{m2i}}{8m^2_{\tilde{d}_{iR}}}\right|^2[f^P_+(s)]^2\lambda_P + \left|\frac{G_F}{\sqrt{2}}V^*_{cd_k} - \sum_i \frac{\lambda'^*_{nki}\tilde{\lambda}'_{m2i}}{8m^2_{\tilde{d}_{iR}}}\right. \\ &\left. + \sum_i \frac{\lambda^*_{inm}\tilde{\lambda}'_{i2k}}{4m^2_{\tilde{\ell}_{iL}}}\frac{s}{m_{\ell_m}(\bar{m}_c - \bar{m}_{d_k})}\right|^2 m^2_{\ell_m}[f^P_0(s)]^2\frac{(m^2_D - m^2_P)^2}{s}, \end{aligned} \tag{14}$$

$$\begin{aligned}N^P_1 &= \left\{\left|\frac{G_F}{\sqrt{2}}V^*_{cd_k} - \sum_i \frac{\lambda'^*_{nki}\tilde{\lambda}'_{m2i}}{8m^2_{\tilde{d}_{iR}}}\right|^2 + Re\left[\left(\frac{G_F}{\sqrt{2}}V^*_{cd_k} - \sum_i \frac{\lambda'^*_{nki}\tilde{\lambda}'_{m2i}}{8m^2_{\tilde{d}_{iR}}}\right)^\dagger\right.\right. \\ &\left.\left. \times \sum_i \frac{\lambda^*_{inm}\tilde{\lambda}'_{i2k}}{4m^2_{\tilde{\ell}_{iL}}}\frac{s}{m_{\ell_m}(\bar{m}_c - \bar{m}_{d_k})}\right]\right\} 2m^2_{\ell_m} f^P_0(s) f^P_+(s)\sqrt{\lambda_P}\frac{(m^2_D - m^2_P)}{s}, \end{aligned} \tag{15}$$

$$N^P_2 = -\left|\frac{G_F}{\sqrt{2}}V^*_{cd_k} - \sum_i \frac{\lambda'^*_{nki}\tilde{\lambda}'_{m2i}}{8m^2_{\tilde{d}_{iR}}}\right|^2[f^P_+(s)]^2\lambda_P\left(1 - \frac{m^2_{\ell_m}}{s}\right), \tag{16}$$

where θ is the angle between the momentum of D meson and the charged lepton in the c.m. system of $\ell-\nu$, and the kinematic factor $\lambda_P = m_D^4 + m_P^4 + s^2 - 2m_D^2 m_P^2 - 2m_D^2 s - 2m_P^2 s$.

Here, we give the definition of the normalized forward-backward (FB) asymmetry of charged lepton, which is more useful from the experimental point of view,

$$\bar{\mathcal{A}}_{FB} = \frac{\int_0^{+1} \frac{d^2\mathcal{B}}{dsdcos\theta} dcos\theta - \int_{-1}^{0} \frac{d^2\mathcal{B}}{dsdcos\theta} dcos\theta}{\int_0^{+1} \frac{d^2\mathcal{B}}{dsdcos\theta} dcos\theta + \int_{-1}^{0} \frac{d^2\mathcal{B}}{dsdcos\theta} dcos\theta}. \tag{17}$$

Explicitly, for $D \to P\ell^+\nu_\ell$ the normalized FB asymmetry is

$$\bar{\mathcal{A}}_{FB}(D \to P\ell^+\nu_\ell) = \frac{N_1^P}{2N_0^P + 2/3N_2^P}. \tag{18}$$

2.3 $D \to V\ell^+\nu_l$ $(V = \rho, K^*, \phi)$ decays

From Eq.(5), $D \to V\ell^+\nu_\ell$ decay amplitude can be written as

$$\begin{aligned}
\mathcal{M}^{\not R_p}(D \to V\ell_m^+\nu_{\ell_n}) &= \left\langle V\ell_m^+\nu_{\ell_n}|\mathcal{H}_{eff}(\bar{c} \to \bar{d}_k\ell_m^+\nu_{\ell_n})|D\right\rangle \\
&= \left[\frac{G_F}{\sqrt{2}}V_{cd_k}^* - \sum_i \frac{\lambda'^*_{nki}\tilde{\lambda}'_{m2i}}{8m^2_{\tilde{d}_{iR}}}\right]\left\langle V|\bar{d}_k\gamma_\mu(1-\gamma_5)c|D\right\rangle(\bar{\nu}_{\ell_n}\gamma^\mu(1-\gamma_5)\ell_m) \\
&\quad + \sum_i \frac{\lambda^*_{inm}\tilde{\lambda}'_{i2k}}{4m^2_{\tilde{\ell}_{iL}}}\left\langle V|\bar{d}_k(1-\gamma_5)c|D\right\rangle(\bar{\nu}_{\ell_n}(1+\gamma_5)\ell_m).
\end{aligned} \tag{19}$$

In terms of the $D \to V$ form factors [43]

$$\begin{aligned}
c_V\left\langle V(p,\varepsilon^*)\left|\bar{d}_k\gamma_\mu(1-\gamma_5)c\right|D(p_D)\right\rangle &= \frac{2V^V(s)}{m_D+m_V}\epsilon_{\mu\nu\alpha\beta}\varepsilon^{*\nu}p_D^\alpha p^\beta \\
&\quad -i\left[\varepsilon_\mu^*(m_D+m_V)A_1^V(s) - (p_D+p)_\mu(\varepsilon^*.p_D)\frac{A_2^V(s)}{m_D+m_V}\right] \\
&\quad +iq_\mu(\varepsilon^*.p_D)\frac{2m_V}{s}[A_3^V(s) - A_0^V(s)],
\end{aligned} \tag{20}$$

$$c_V\left\langle V(p,\varepsilon^*)\left|\bar{d}_k\gamma_5 c\right|D(p_D)\right\rangle = -i\frac{\varepsilon^*.p_D}{m_D}\frac{2m_Dm_V}{\bar{m}_c+\bar{m}_{d_k}}A_0^V(s), \tag{21}$$

where $c_V = \sqrt{2}$ for ρ^0, $c_V = 1$ for $\rho^-, K^{*0}, K^{*-}, \phi$ and with the relation $A_3^V(s) = \frac{m_D+m_V}{2m_V}A_1^V(s) - \frac{m_D-m_V}{2m_V}A_2^V(s)$ and $A_0^V(s) = A_3^V(s) - A_3'^V(s)$, we have

$$\frac{d\mathcal{B}^{\not R_p}(D \to V\ell_m^+\nu_{\ell_n})}{dsdcos\theta} = \frac{\tau_D\sqrt{\lambda_V}}{2^7\pi^3m_D^3c_V^2}\left(1-\frac{m_{\ell_m}^2}{s}\right)^2\left[N_0^V + N_1^V cos\theta + N_2^V cos^2\theta\right], \tag{22}$$

with

$$N_0^V = \left|\frac{G_F}{\sqrt{2}}V_{cd_k}^* - \sum_i \frac{\lambda'^*_{nki}\tilde{\lambda}'_{m2i}}{8m^2_{\tilde{d}_{iR}}}\right|^2\left\{[A_1^V(s)]^2\left(\frac{\lambda_V}{4m_V^2} + (m_{\ell_m}^2+2s)\right)(m_D+m_V)^2\right.$$

$$
\begin{aligned}
&+[A_2^V(s)]^2\frac{\lambda_V^2}{4m_V^2(m_D+m_V)^2}+[V^V(s)]^2\frac{\lambda_V}{(m_D+m_V)^2}(m_{\ell_m}^2+s)\\
&-A_1^V(s)A_2^V(s)\frac{\lambda_V}{2m_V^2}(m_D^2-s-m_V^2)\Bigg\}\\
&+\left|\frac{G_F}{\sqrt{2}}V_{cd_k}^*-\sum_i\frac{\lambda'^*_{nki}\tilde{\lambda}'_{m2i}}{8m^2_{\tilde{d}_{iR}}}+\sum_i\frac{\lambda^*_{inm}\tilde{\lambda}'_{i2k}}{4m^2_{\tilde{\ell}_{iL}}}\frac{s}{m_{\ell_m}(\bar{m}_c+\bar{m}_{d_k})}\right|^2[A_0^v(s)]\frac{m_{\ell_m}^2}{s}\lambda_V, \qquad (23)
\end{aligned}
$$

$$
\begin{aligned}
N_1^V &= \Bigg\{\left|\frac{G_F}{\sqrt{2}}V_{cd_k}^*-\sum_i\frac{\lambda'^*_{nki}\tilde{\lambda}'_{m2i}}{8m^2_{\tilde{d}_{iR}}}\right|^2\\
&+Re\left[\left(\frac{G_F}{\sqrt{2}}V_{cd_k}^*-\sum_i\frac{\lambda'^*_{nki}\tilde{\lambda}'_{m2i}}{8m^2_{\tilde{d}_{iR}}}\right)^\dagger\sum_i\frac{\lambda^*_{inm}\tilde{\lambda}'_{i2k}}{4m^2_{\tilde{\ell}_{iL}}}\frac{s}{m_{\ell_m}(\bar{m}_c-\bar{m}_{d_k})}\right]\Bigg\}\\
&\times\left[A_0^V(s)A_1^V(s)\frac{m_{\ell_m}^2(m_D+m_V)(m_D^2-m_V^2-s)\sqrt{\lambda_V}}{sm_V}-A_0^V(s)A_2^V(s)\frac{m_{\ell_m}^2\lambda_V^{\frac{3}{2}}}{sm_V(m_D+m_V)}\right]\\
&+\left|\frac{G_F}{\sqrt{2}}V_{cd_k}^*-\sum_i\frac{\lambda'^*_{nki}\tilde{\lambda}'_{m2i}}{8m^2_{\tilde{d}_{iR}}}\right|^2A_1^V(s)V^V(s)4s\sqrt{\lambda_V}, \qquad (24)\\
N_2^V &= -\left|\frac{G_F}{\sqrt{2}}V_{cd_k}^*-\sum_i\frac{\lambda'^*_{nki}\tilde{\lambda}'_{m2i}}{8m^2_{\tilde{d}_{iR}}}\right|^2\left(1-\frac{m_{\ell_m}^2}{s}\right)\lambda_V\Bigg\{[A_1^V(s)]^2\frac{(m_D+m_V)^2}{4m_V^2}+[V^V(s)]^2\frac{s}{(m_D+m_V)^2}\\
&+[A_2^V(s)]^2\frac{\lambda_V}{4m_V^2(m_D+m_V)^2}-A_1^V(s)A_2^V(s)\frac{m_D^2-m_V^2-s}{2m_V^2}\Bigg\}, \qquad (25)
\end{aligned}
$$

where $\lambda_V=m_D^4+m_V^4+s^2-2m_D^2m_V^2-2m_D^2s-2m_V^2s$.

The normalized FB asymmetry of $D\to V\ell^+\nu_\ell$ can be written as

$$
\bar{\mathcal{A}}_{FB}(D\to V\ell^+\nu_\ell)=\frac{N_1^V}{2N_0^V+2/3N_2^V}. \qquad (26)
$$

3 Numerical Results and Discussions

In this section, we summarize our numerical results and analysis of RPV couplings in the exclusive $\bar{c}\to\bar{d}/\bar{s}\ell^+\nu_\ell$ decays. When we study the effects due to SUSY without R-parity, we consider only one new coupling at one time, neglecting the interferences between different new couplings, but keeping their interferences with the SM amplitude. The input parameters are collected in the Appendix. To be conservative, the input parameters varied randomly within 1σ variance and the experimental bounds at 90% confidence level (CL) will be used to constrain parameters of the relevant new couplings.

3.1 The exclusive $\bar{c} \to \bar{d}e^+\nu_e$ decays

There are two RPV coupling products, $\lambda^*_{i11}\tilde{\lambda}'_{i21}$ due to slepton exchange and $\lambda'^*_{11i}\tilde{\lambda}'_{12i}$ due to squark exchange, contributing to seven exclusive $\bar{c} \to \bar{d}e^+\nu_e$ decay modes, $D_d^+ \to e^+\nu_e$, $D_u^0 \to \pi^- e^+\nu_e$, $D_d^+ \to \pi^0 e^+\nu_e$, $D_s^+ \to K^0 e^+\nu_e$, $D_u^0 \to \rho^- e^+\nu_e$, $D_d^+ \to \rho^0 e^+\nu_e$ and $D_s^+ \to K^{*0} e^+\nu_e$. All relevant semilpetonic branching ratios of the exclusive $\bar{c} \to \bar{d}e^+\nu_e$ decays have been accurately measured by BSEIII [1–3], CLEO-c [5–8] and Belle [13], furthermore, the pureleptonic branching ratios of $D_d^+ \to e^+\nu_e$ is upperlimited by CLEO-c [9]. Their average values from PDG [44] and corresponding experimental bound at 90% CL are given in the second column of Table 1. Moreover, the SM prediction values with 1σ error ranges for the input parameters are listed in the third column of Table 1. The theoretical predictions of relevant branching fractions are consistent with experimental data at the present level of precision, and we can constrain the relevant NP parameter spaces by these D decays.

Our bounds for $\lambda^*_{i11}\tilde{\lambda}'_{i21}$ and $\lambda'^*_{11i}\tilde{\lambda}'_{12i}$ from the 90% CL experimental data are demonstrated in Fig. 2. We can see that the moduli of both $\lambda^*_{i11}\tilde{\lambda}'_{i21}$ and $\lambda'^*_{11i}\tilde{\lambda}'_{12i}$ as well as the RPV weak phase of $\lambda'^*_{11i}\tilde{\lambda}'_{12i}$ are constrained by current experimental measurements. We get $|\lambda^*_{i11}\tilde{\lambda}'_{i21}| \leq 1.15 \times 10^{-2}$ and $|\lambda'^*_{11i}\tilde{\lambda}'_{12i}| \leq 7.66$. The bound on slepton exchange coupling $\lambda^*_{i11}\tilde{\lambda}'_{i21}$ is derived for the first time. Squark exchange coupling $\tilde{\lambda}'^*_{11i}\tilde{\lambda}'_{12i}$ gives contribution to $c \to ue^+e^-$ transition and $D^0 - \bar{D}^0$ mixing. There are much stronger bounds from $c \to ue^+e^-$ transition and $D^0 - \bar{D}^0$ mixing, which are $|\tilde{\lambda}'^*_{11i}\tilde{\lambda}'_{12i}| \leq 4.5 \times 10^{-2}$

Table 1: Branching ratios of the exclusive $\bar{c} \to \bar{d}e^+\nu_e$ decays are in units of 10^{-3} except for branching ratio of $D_d^+ \to e^+\nu_e$ is in units of 10^{-8}. "a" denotes the experimental data and "b" denotes the corresponding experimental bound at 90% CL.

Observable	Exp. data	SM predictions	SUSY w/$\lambda^*_{i11}\tilde{\lambda}'_{i21}$	SUSY w/$\lambda'^*_{11i}\tilde{\lambda}'_{12i}$
$\mathcal{B}(D_d^+ \to e^+\nu_e)$	< 880	$[0.71, 1.02]$	< 880	$[0.49, 1.24]$
$\mathcal{B}(D_u^0 \to \pi^- e^+\nu_e)$	$(2.89\pm0.08)^a$ $[2.76,\ 3.02]^b$	$[1.86, 6.37]$	$[2.89, 3.02]$	$[2.90, 3.02]$
$\mathcal{B}(D_d^+ \to \pi^0 e^+\nu_e)$	$(4.05\pm0.18)^a$ $[3.75,\ 4.35]^b$	$[2.39, 8.21]$	$[3.75, 3.92]$	$[3.75, 3.91]$
$\mathcal{B}(D_s^+ \to K^0 e^+\nu_e)$	$(3.7\pm1.0)^a$ $[2.06,\ 5.34]^b$	$[2.36, 5.32]$	$[2.36, 5.32]$	$[2.06, 5.34]$
$\mathcal{B}(D_u^0 \to \rho^- e^+\nu_e)$	$(1.9\pm0.4)^a$ $[1.24,\ 2.56]^b$	$[1.49, 2.10]$	$[1.49, 2.10]$	$[1.24, 2.21]$
$\mathcal{B}(D_d^+ \to \rho^0 e^+\nu_e)$	$(2.2\pm0.4)^a$ $[1.54,\ 2.86]^b$	$[1.93, 2.72]$	$[1.93, 2.72]$	$[1.60, 2.86]$
$\mathcal{B}(D_s^+ \to K^{*0} e^+\nu_e)$	$(1.8\pm0.7)^a$ $[0.65,\ 2.95]^b$	$[1.92, 2.74]$	$[1.92, 2.74]$	$[1.35, 2.92]$

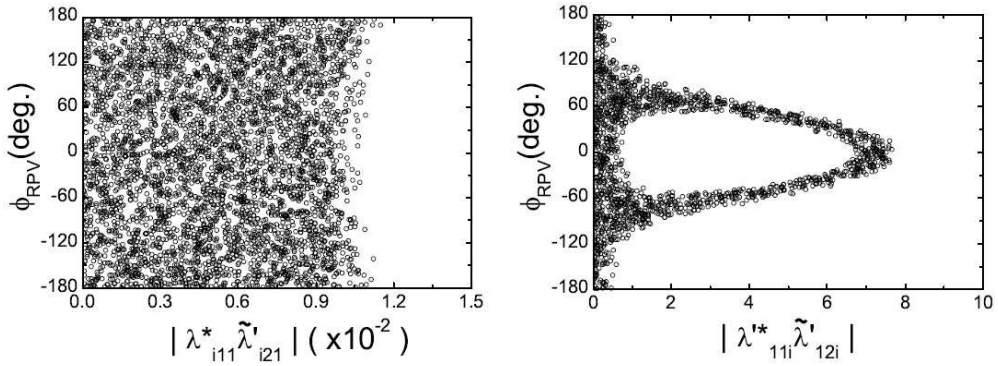

Figure 2: The allowed RPV parameter spaces from the exclusive $\bar{c} \to \bar{d}e^+\nu_e$ decays at 90% CL with 500 GeV sfermion mass.

from $c \to ue^+e^-$ transition [45] and $|\tilde{\lambda}'^*_{11i}\tilde{\lambda}'_{12i}| \leq 1.0 \times 10^{-2}$ from $D^0 - \bar{D}^0$ lifetime difference [36]. If neglecting the difference between λ' and $\tilde{\lambda}'$, our bound on $\lambda'^*_{11i}\tilde{\lambda}'_{12i}$ from $\bar{c} \to \bar{d}e^+\nu_e$ is more than two orders weaker than one from $c \to ue^+e^-$ transition or $D^0 - \bar{D}^0$ mixing.

Now we will analyze the constrained RPV effects in the exclusive $\bar{c} \to \bar{d}e^+\nu_e$ decays. Using the constrained parameter spaces shown in Fig. 2, we can predict the constrained RPV effects on the branching ratios, the differential branching ratios and the normalized FB asymmetries of charged leptons. The numerical results for the branching ratios are listed in the last two columns of Table 1, and the constrained RPV effects of $\lambda^*_{i11}\tilde{\lambda}'_{i21}$ and $\lambda'^*_{11i}\tilde{\lambda}'_{12i}$ in the exclusive $\bar{c} \to \bar{d}e^+\nu_e$ decays are displayed in Fig. 3 and Fig. 4, respectively. Comparing the RPV SUSY predictions to the SM ones or experimental bounds given in Table 1 as well as shown in Fig. 3 and Fig. 4, we give some remarks as follows.

For the slepton exchange coupling $\lambda^*_{i11}\tilde{\lambda}'_{i21}$, since its contribution to $\mathcal{B}(D_d^+ \to e^+\nu_e)$ is increased by m_D/m_e, as shown in Fig. 3 (a-b), $\mathcal{B}(D_d^+ \to e^+\nu_e)$ can be extremely enhanced or reduced by the constrained $\lambda^*_{i11}\tilde{\lambda}'_{i21}$ coupling, and it is very sensitve to both modulus and weak phase of $\lambda^*_{i11}\tilde{\lambda}'_{i21}$, furthermore, $|\lambda^*_{i11}\tilde{\lambda}'_{i21}|$ is tightly upper-limited by the experimental measurement of $\mathcal{B}(D_d^+ \to e^+\nu_e)$. The constrained slepton exchange coupling $\lambda^*_{i11}\tilde{\lambda}'_{i21}$ has no obvious contribution to the six semileptonic decay branching ratios. From the forth column of Table 1, one can find that present accurate experimental measurements of $\mathcal{B}(D_u^0 \to \pi^- e^+\nu_e)$ and $\mathcal{B}(D_d^+ \to \pi^0 e^+\nu_e)$ give very strong bounds on the semileptonic decay branching ratio predictions with $\lambda^*_{i11}\tilde{\lambda}'_{i21}$ coupling. As for the differential branching ratios and the normalized FB asymmetries of relevant semileptonic D decays, slepton exchange RPV contributions to $D_u^0 \to \pi^- e^+\nu_e$, $D_d^+ \to \pi^0 e^+\nu_e$ and $D_s^+ \to K^0 e^+\nu_e$ ($D_u^0 \to \rho^- e^+\nu_e$, $D_d^+ \to \rho^0 e^+\nu_e$ and $D_s^+ \to K^{*0} e^+\nu_e$) are very similar to each other. We would take $D_u^0 \to \pi^- e^+\nu_e$ and

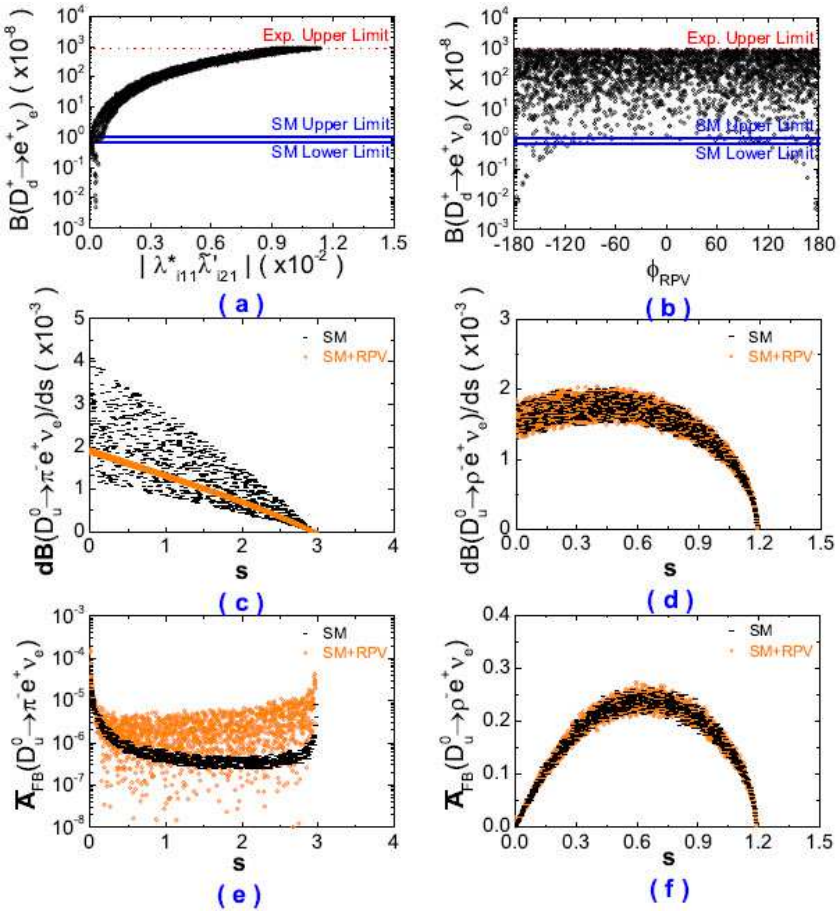

Figure 3: The constrained effects of RPV coupling $\lambda^*_{i11}\tilde{\lambda}'_{i21}$ due to the slepton exchange in the exclusive $\bar{c} \to \bar{d}e^+\nu_e$ decays.

$D_u^0 \to \rho^- e^+\nu_e$ as examples (the similar in the subsections of the exclusive $\bar{c} \to \bar{d}\mu^+\nu_\mu, \bar{s}e^+\nu_e, \bar{s}\mu^+\nu_\mu$ decays), which are shown by Fig. 3 (c,e) and Fig. 3 (d,f), respectively. We can see that present accurate experimental measurements of $\mathcal{B}(D_u^0 \to \pi^- e^+\nu_e)$ and $\mathcal{B}(D_d^+ \to \pi^0 e^+\nu_e)$ also give very strong bounds on their differential branching ratios, nevertheless, other differential branching ratios (including $d\mathcal{B}(D_s^+ \to K^0 e^+\nu_e)/ds$) are not constrained so much by present experimental measurements given in Table 1. The RPV predictions of the four differential branching ratios of $D_s^+ \to K^0 e^+\nu_e$, $D_u^0 \to \rho^- e^+\nu_e$, $D_d^+ \to \rho^0 e^+\nu_e$ and $D_s^+ \to K^{*0} e^+\nu_e$ decays can not be distinguished from their SM ones at all s range. As displayed in Fig. 3 (e), the constrained slepton exchange coupling has quite large effects on the normalized FB asymmetries of $D_u^0 \to \pi^- e^+\nu_e$, $D_d^+ \to \pi^0 e^+\nu_e$ and $D_s^+ \to K^0 e^+\nu_e$ decays, but these values are very tiny.

The contributions of the squark exchange coupling $\lambda'^*_{11i}\tilde{\lambda}'_{12i}$ are totally different to ones of the slepton exchange coupling $\lambda^*_{i11}\tilde{\lambda}'_{i21}$. Our constrained $\lambda'^*_{11i}\tilde{\lambda}'_{12i}$ has small effects on $\mathcal{B}(D_d^+ \to e^+\nu_e)$, but

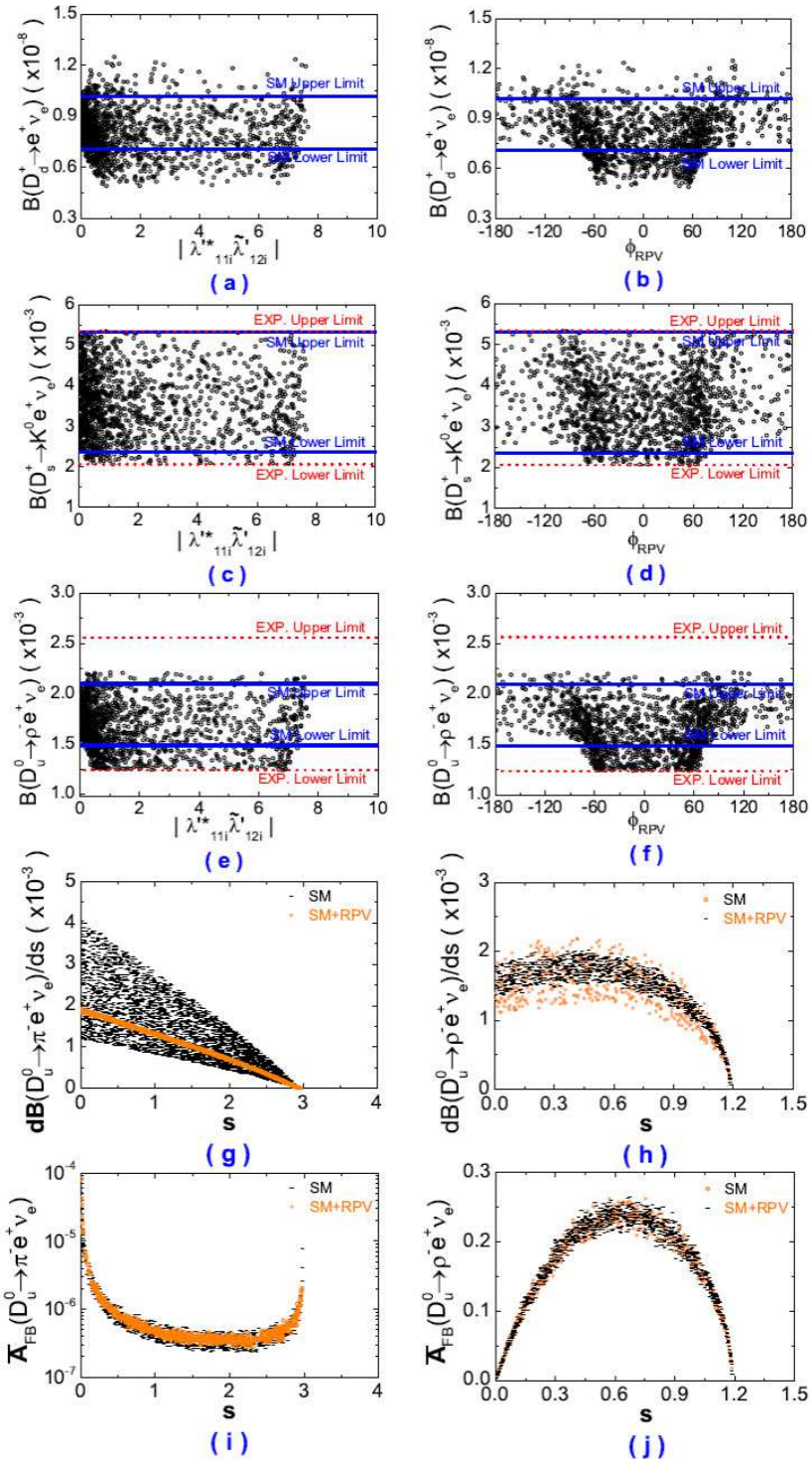

Figure 4: The constrained effects of RPV coupling $\lambda'^{*}_{11i}\tilde{\lambda}'_{12i}$ due to the squark exchange in the exclusive $\bar{c} \to \bar{d}e^{+}\nu_e$ decays.

it has obvious effects in the six semileptonic D decays. From the last column of Table 1, one can see that the experimental measurements of all relevant semileptonic D decays except $D_s^+ \to K^{*0}e^+\nu_e$ give bounds on $\lambda'^*_{11i}\tilde{\lambda}'_{12i}$. Except $\mathcal{B}(D_u^0 \to \pi^- e^+\nu_e)$ and $\mathcal{B}(D_d^+ \to \pi^0 e^+\nu_e)$, which are strongly constrained by their experimental measurements, as shown in Fig. 4 (a-f), all other branching ratios are sensitive to both modulus and weak phase of $\lambda'^*_{11i}\tilde{\lambda}'_{12i}$. Note that $\mathcal{B}(D_d^+ \to e^+\nu_e)$ including the constrained $\lambda'^*_{11i}\tilde{\lambda}'_{12i}$ is much less than its experimental upper limit, therefore we do not show the experimental upper limit in Fig. 4 (a-b). The constrained squark exchange contributions to the differential branching ratios and the normalized FB asymmetries of $D_u^0 \to \pi^- e^+\nu_e$, $D_d^+ \to \pi^0 e^+\nu_e$ and $D_s^+ \to K^0 e^+\nu_e$ ($D_u^0 \to \rho^- e^+\nu_e$, $D_d^+ \to \rho^0 e^+\nu_e$ and $D_s^+ \to K^{*0} e^+\nu_e$) are very similar to each other. We would also take $D_u^0 \to \pi^- e^+\nu_e$ and $D_u^0 \to \rho^- e^+\nu_e$ as examples (the similar in the subsections of the exclusive $\bar{c} \to \bar{d}\mu^+\nu_\mu, \bar{s}e^+\nu_e, \bar{s}\mu^+\nu_\mu$ decays), which are displayed in Fig. 4 (g-j). Fig. 4 (h-i) show us that our constrained $\lambda'^*_{11i}\tilde{\lambda}'_{12i}$ coupling could enlarge the allowed ranges of $d\mathcal{B}(D_u^0 \to \rho^- e^+\nu_e)$, but it could shrink the allowed ranges of $\bar{A}_{FB}(D_u^0 \to \pi^- e^+\nu_e)$. Noted that, if considering the further constraints from $D^0 - \bar{D}^0$ mixing and $c \to ue^+e^-$ transition, i.e., $|\tilde{\lambda}'^*_{11i}\tilde{\lambda}'_{12i}| \leq 1.0 \times 10^{-2}$, the further constrained $\lambda'^*_{11i}\tilde{\lambda}'_{12i}$ coupling has small effects in the exclusive $\bar{c} \to \bar{d}e^+\nu_e$ decays.

3.2 The exclusive $\bar{c} \to \bar{d}\mu^+\nu_\mu$ decays

Two RPV coupling products, $\lambda^*_{i22}\tilde{\lambda}'_{i21}$ due to slepton exchange and $\lambda'^*_{21i}\tilde{\lambda}'_{22i}$ due to squark exchange, contribute to seven exclusive $\bar{c} \to \bar{d}\mu^+\nu_\mu$ decay modes, $D_d^+ \to \mu^+\nu_\mu$, $D_u^0 \to \pi^-\mu^+\nu_\mu$, $D_d^+ \to \pi^0\mu^+\nu_\mu$, $D_s^+ \to K^0\mu^+\nu_\mu$, $D_u^0 \to \rho^-\mu^+\nu_\mu$, $D_d^+ \to \rho^0\mu^+\nu_\mu$ and $D_s^+ \to K^{*0}\mu^+\nu_\mu$. Three relevant branching ratios of the exclusive $\bar{c} \to \bar{d}\mu^+\nu_\mu$ decays have been measured by BESIII [4], CLEO-c [8, 9], Belle [13] and BES [18], and their average values from PDG [44] and corresponding experimental bound at 90% CL are given in the second column of Table 2. The SM prediction values with 1σ error ranges for the input parameters are listed in the third column of Table 2.

Our bounds for $\lambda^*_{i22}\tilde{\lambda}'_{i21}$ and $\lambda'^*_{21i}\tilde{\lambda}'_{22i}$ from the 90% CL experimental data are demonstrated in Fig. 5, and both modulus and weak phase of $\lambda^*_{i22}\tilde{\lambda}'_{i21}$ are strongly constrained by the experimental measurements of $\mathcal{B}(D_u^0 \to \pi^-\mu^+\nu_\mu)$, and $\lambda'^*_{21i}\tilde{\lambda}'_{22i}$ is constrained by the experimental measurements of $\mathcal{B}(D_u^0 \to \pi^-\mu^+\nu_\mu)$ as well as $\mathcal{B}(D_d^+ \to \rho^0\mu^+\nu_\mu)$. We get $|\lambda^*_{i22}\tilde{\lambda}'_{i21}| \leq 1.46 \times 10^{-1}$ and $|\lambda'^*_{21i}\tilde{\lambda}'_{22i}| \leq 7.89$. The bound on slepton exchange coupling $\lambda^*_{i22}\tilde{\lambda}'_{i21}$ is derived for the first time. Squark exchange coupling $\tilde{\lambda}'^*_{21i}\tilde{\lambda}'_{22i}$ could give contribution to $c \to u\mu^+\mu^-$ transition and $D^0 - \bar{D}^0$ mixing. There are much stronger bounds from $c \to u\mu^+\mu^-$ transition and $D^0 - \bar{D}^0$ mixing, which are $|\tilde{\lambda}'^*_{21i}\tilde{\lambda}'_{22i}| \leq 1.25 \times 10^{-2}$ from $c \to u\mu^+\mu^-$ transition [45] and $|\tilde{\lambda}'^*_{21i}\tilde{\lambda}'_{22i}| \leq 7.25 \times 10^{-2}$ from $D^0 - \bar{D}^0$ lifetime difference [36]. If

Table 2: Branching ratios of the exclusive $\bar{c} \to \bar{d}\mu^+\nu_\mu$ decays (in units of 10^{-3}) except for $\mathcal{B}(D_d^+ \to \mu^+\nu_\mu)$ (in units of 10^{-4}). "a" denotes the experimental data and "b" denotes the corresponding experimental bound at 90% CL.

Observable	Exp. data	SM predictions	SUSY w/$\lambda^*_{i22}\tilde{\lambda}'_{i21}$	SUSY w/$\lambda'^*_{21i}\tilde{\lambda}'_{22i}$
$\mathcal{B}(D_d^+ \to \mu^+\nu_\mu)$	$(3.82\pm0.33)^a$ $[3.28,\ 4.36]^b$	$[3.02, 4.32]$	$[3.38, 4.10]$	$[3.38, 4.10]$
$\mathcal{B}(D_u^0 \to \pi^-\mu^+\nu_\mu)$	$(2.37\pm0.24)^a$ $[1.98,\ 2.76]^b$	$[1.88, 6.17]$	$[1.98, 2.76]$	$[1.98, 2.76]$
$\mathcal{B}(D_d^+ \to \pi^0\mu^+\nu_\mu)$	$\cdots$	$[2.42, 7.92]$	$[2.53, 3.58]$	$[2.53, 3.58]$
$\mathcal{B}(D_s^+ \to K^0\mu^+\nu_\mu)$	$\cdots$	$[2.40, 5.19]$	$[2.32, 5.16]$	$[1.99, 6.68]$
$\mathcal{B}(D_u^0 \to \rho^-\mu^+\nu_\mu)$	$\cdots$	$[1.55, 2.15]$	$[1.52, 2.17]$	$[1.35, 2.37]$
$\mathcal{B}(D_d^+ \to \rho^0\mu^+\nu_\mu)$	$(2.4\pm0.4)^a$ $[1.74,\ 3.06]^b$	$[2.01, 2.79]$	$[1.97, 2.81]$	$[1.74, 3.06]$
$\mathcal{B}(D_s^+ \to K^{*0}\mu^+\nu_\mu)$	$\cdots$	$[1.99, 2.79]$	$[2.00, 2.80]$	$[1.67, 3.45]$

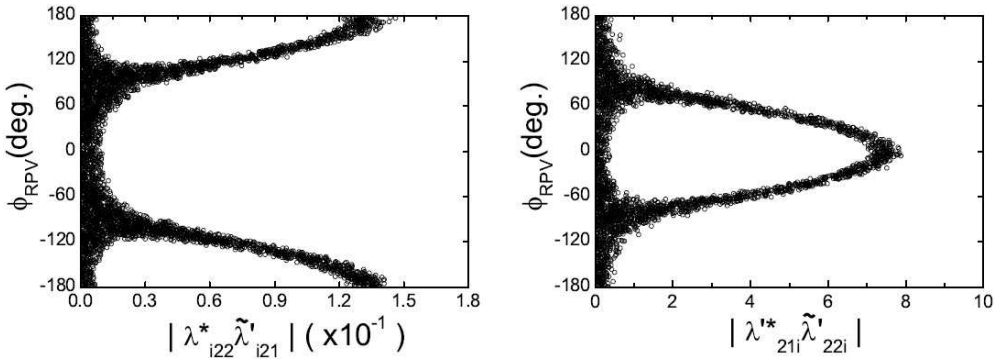

Figure 5: The allowed RPV parameter spaces from the exclusive $\bar{c} \to \bar{d}\mu^+\nu_\mu$ decays at 90% CL with 500 GeV sfermion mass.

neglecting the difference between λ' and $\tilde{\lambda}'$, our bound on $\lambda'^*_{21i}\tilde{\lambda}'_{22i}$ from $\bar{c} \to \bar{d}\mu^+\nu_\mu$ is much weaker than one from $c \to u\mu^+\mu^-$ transition or $D^0 - \bar{D}^0$ mixing.

Now we discuss the constrained RPV effects in the exclusive $\bar{c} \to \bar{d}\mu^+\nu_\mu$ decays. The numerical results for the branching ratios are listed in the last two columns of Table 2, and the constrained RPV effects of $\lambda^*_{i22}\tilde{\lambda}'_{i21}$ and $\lambda'^*_{21i}\tilde{\lambda}'_{22i}$ in the exclusive $\bar{c} \to \bar{d}\mu^+\nu_\mu$ decays are shown in Fig. 6 and Fig. 7, respectively. We have the following remarks for the constrained RPV effects.

For the slepton exchange coupling $\lambda^*_{i22}\tilde{\lambda}'_{i21}$, since all seven relevant branching ratios are not sensitive to both modulus and weak phase of the constrained $\lambda^*_{i22}\tilde{\lambda}'_{i21}$ coupling, we do not show them in Fig. 6.

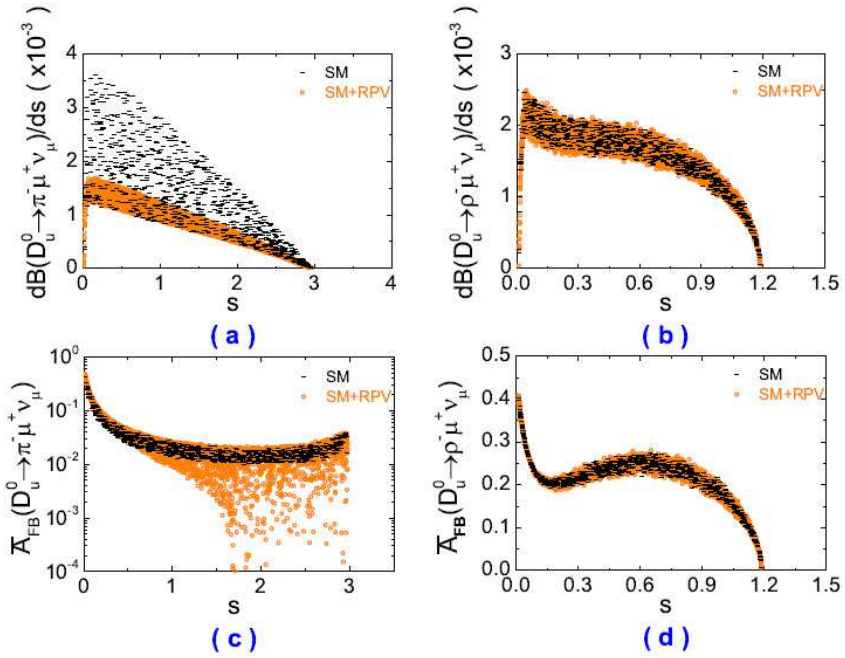

Figure 6: The constrained effects of RPV coupling $\lambda^*_{i22}\tilde{\lambda}'_{i21}$ due to the slepton exchange in the exclusive $\bar{c} \to \bar{d}\mu^+\nu_\mu$ decays.

From the forth column of Table 2 and Fig. 6 (a-b), one can find that present accurate experimental measurements of $\mathcal{B}(D^0_u \to \pi^-\mu^+\nu_\mu)$ give very strong bounds on the branching ratios and the differential branching ratios of $D^0_u \to \pi^-\mu^+\nu_\mu$ and $D^+_d \to \pi^0\mu^+\nu_\mu$ decays, but it does not give obvious bound on other branching ratios and differential branching ratios. As shown in Fig. 6 (c), the constrained $\lambda^*_{i22}\tilde{\lambda}'_{i21}$ coupling could have great effects on $\mathcal{A}_{FB}(D^0_u \to \pi^-\mu^+\nu_\mu, D^+_d \to \pi^0\mu^+\nu_\mu, D^0{+_s} \to K^0\mu^+\nu_\mu)$ at the middle and high s region, nevertheless, Fig. 6 (d) shows us the constrained $\lambda^*_{i22}\tilde{\lambda}'_{i21}$ coupling has no obvious effect on $\mathcal{A}_{FB}(D^0_u \to \rho^-\mu^+\nu_\mu, D^+_d \to \rho^0\mu^+\nu_\mu, D^+_s \to K^*\mu^+\nu_\mu)$.

As for the squark exchange coupling $\lambda'^*_{21i}\tilde{\lambda}'_{22i}$, the examples of the branching ratios are shown in Fig. 7 (a-d), relevant semileptonic branching ratios expect $\mathcal{B}(D^0_u \to \pi^-\mu^+\nu_\mu)$ and $\mathcal{B}(D^+_d \to \pi^0\mu^+\nu_\mu)$ are sensitive to both modulus and weak phase of $\lambda'^*_{21i}\tilde{\lambda}'_{22i}$, and these branching ratios could have minimum at $\phi_{RPV} \in [-70°, 70°]$. From Fig. 7 (e-f), we can see that the constrained $\lambda'^*_{21i}\tilde{\lambda}'_{22i}$ coupling let $\mathcal{B}(D^0_u \to \pi^-\mu^+\nu_\mu)$ and $\mathcal{B}(D^+_d \to \pi^0\mu^+\nu_\mu)$ close to their SM lower limits, and could enlarge the allowed ranges of other four semileptonic differential branching ratios. Fig. 7 (g-h) shows us that the constrained $\lambda'^*_{21i}\tilde{\lambda}'_{22i}$ coupling let $\mathcal{A}_{FB}(D^0_u \to \pi^-\mu^+\nu_\mu, D^+_d \to \pi^0\mu^+\nu_\mu, D^+_s \to K^0\mu^+\nu_\mu)$ close to their SM upper limits, but has no very obvious effect on $\mathcal{A}_{FB}(D^0_u \to \rho^-\mu^+\nu_\mu, D^+_d \to \rho^0\mu^+\nu_\mu, D^+_s \to K^{*0}\mu^+\nu_\mu)$. However, if considering the further constraints from $D^0 - \bar{D}^0$ mixing and $c \to u\mu^+\mu^-$

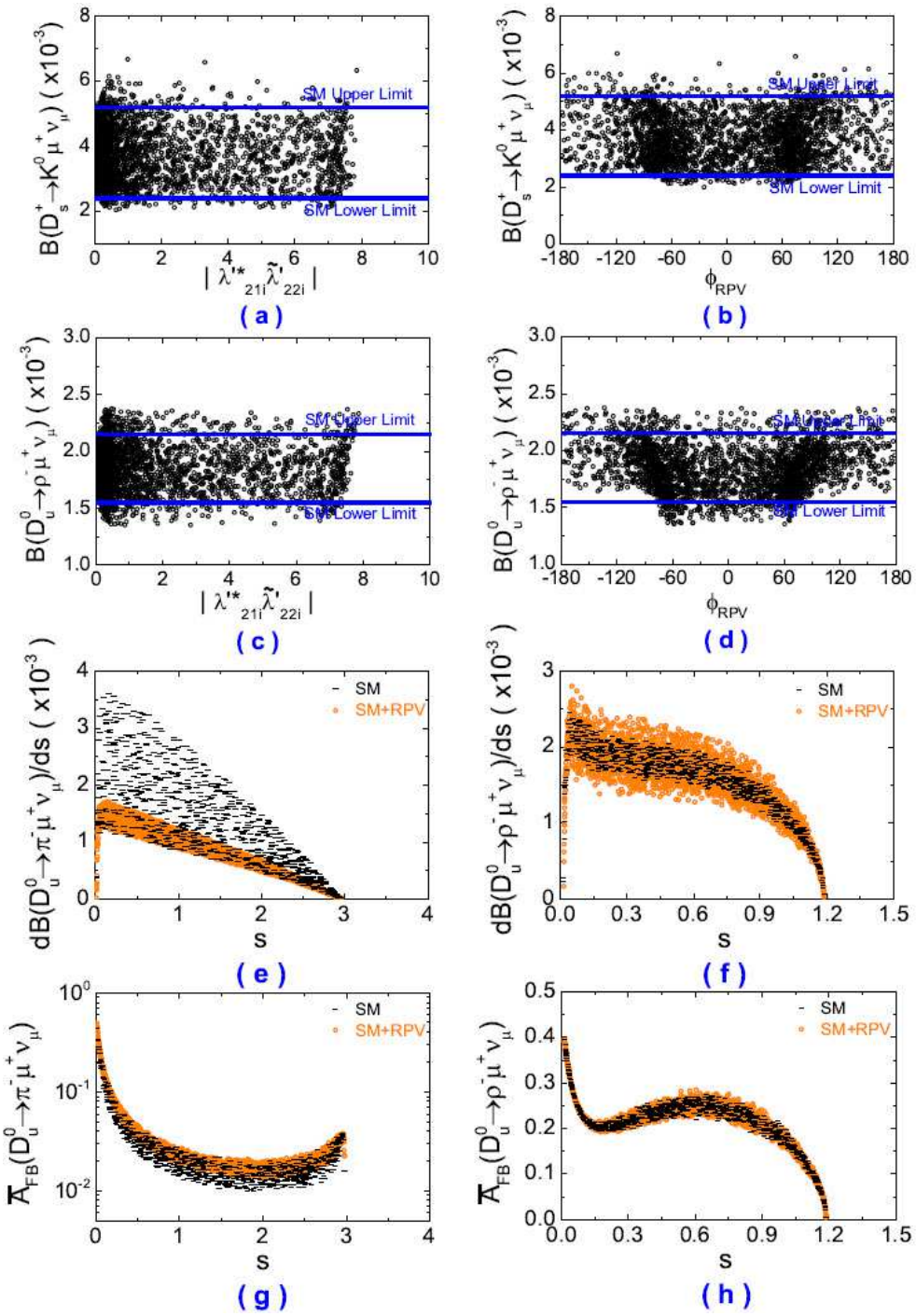

Figure 7: The constrained effects of RPV coupling $\lambda'^{*}_{21i}\tilde{\lambda}'_{22i}$ due to the squark exchange in the exclusive $\bar{c} \to \bar{d}\mu^{+}\nu_{\mu}$ decays.

transition, the further constrained $\lambda'^{*}_{21i}\tilde{\lambda}'_{22i}$ coupling has no obviuos effects in the exclusive $\bar{c} \to \bar{d}\mu^{+}\nu_{\mu}$ decays.

3.3 The exclusive $\bar{c} \to \bar{s}e^+\nu_e$ decays

There are two RPV coupling products, $\lambda^*_{i11}\tilde{\lambda}'_{i22}$ due to slepton exchange and $\lambda'^*_{12i}\tilde{\lambda}'_{12i}$ due to squark exchange, contributing to six exclusive $\bar{c} \to \bar{s}e^+\nu_e$ decay modes, $D_s^+ \to e^+\nu_e$, $D_u^0 \to K^-e^+\nu_e$, $D_d^+ \to K^0e^+\nu_e$, $D_u^0 \to K^{*-}e^+\nu_e$, $D_d^+ \to K^{*0}e^+\nu_e$ and $D_s^+ \to \phi e^+\nu_e$. All relevant semilpetonic branching ratios of the exclusive $\bar{c} \to \bar{s}e^+\nu_e$ decays have been accurately measured and the pureleptonic branching ratios of $D_s^+ \to e^+\nu_e$ has been upperlimited by BESIII [2], CLEO-c [5, 7, 10–12], BABAR [15, 16], BES [20, 21], Belle [13] and MARK-III [23]. Their average values from PDG [44] and corresponding experimental bounds at 90% CL are given in the second column of Table 3. Moreover, the SM prediction values with 1σ error ranges for the input parameters are listed in the third column of Table 3.

Our bounds for $\lambda^*_{i11}\tilde{\lambda}'_{i22}$ and $\lambda'^*_{12i}\tilde{\lambda}'_{12i}$ from the 90% CL experimental data are demonstrated in Fig. 8. We get $|\lambda^*_{i11}\tilde{\lambda}'_{i22}| \leq 4.53 \times 10^{-2}$ and $|\lambda'^*_{12i}\tilde{\lambda}'_{12i}| \leq 33.50$. Noted that both bounds are derived for the first time. We also predict the constrained RPV effects in the exclusive $\bar{c} \to \bar{s}e^+\nu_e$ decays. The numerical results for the branching ratios are listed in the last two columns of Table 3. The constrained RPV effects due to the slepton exchange and squark exchange are displayed in Fig. 9 and Fig. 10, respectively. One can see that the RPV effects in the exclusive $\bar{c} \to \bar{s}e^+\nu_e$ decays are similar to ones in the exclusive $\bar{c} \to \bar{d}e^+\nu_e$ decays.

Table 3: Branching ratios of the exclusive $\bar{c} \to \bar{s}e^+\nu_e$ decays (in units of 10^{-2}) except for $\mathcal{B}(D_s^+ \to e^+\nu_e)$ (in units of 10^{-7}). "a" denotes the experimental data and "b" denotes the corresponding experimental bounds at 90% CL.

Observable	Exp. data	SM predictions	SUSY w/$\lambda^*_{i11}\tilde{\lambda}'_{i22}$	SUSY w/$\lambda'^*_{12i}\tilde{\lambda}'_{12i}$
$\mathcal{B}(D_s^+ \to e^+\nu_e)$	< 1200	$[1.06, 1.44]$	$[0.08, 1200]$	$[1.07, 1.70]$
$\mathcal{B}(D_u^0 \to K^-e^+\nu_e)$	$(3.55\pm0.05)^a$ $[3.47,3.63]^b$	$[2.14, 4.02]$	$[3.47, 3.63]$	$[3.47, 3.63]$
$\mathcal{B}(D_d^+ \to K^0e^+\nu_e)$	$(8.83\pm0.22)^a$ $[8.47,9.19]^b$	$[5.47, 10.23]$	$[8.82, 9.19]$	$[8.82, 9.19]$
$\mathcal{B}(D_u^0 \to K^{*-}e^+\nu_e)$	$(2.16\pm0.16)^a$ $[1.90,2.42]^b$	$[1.72, 2.21]$	$[2.05, 2.21]$	$[2.07, 2.28]$
$\mathcal{B}(D_d^+ \to K^{*0}e^+\nu_e)$	$(5.52\pm0.15)^a$ $[5.27,5.77]^b$	$[4.36, 5.65]$	$[5.27, 5.63]$	$[5.27, 5.77]$
$\mathcal{B}(D_s^+ \to \phi e^+\nu_e)$	$(2.49\pm0.14)^a$ $[2.26,2.72]^b$	$[1.97, 2.95]$	$[2.26, 2.72]$	$[2.26, 2.72]$

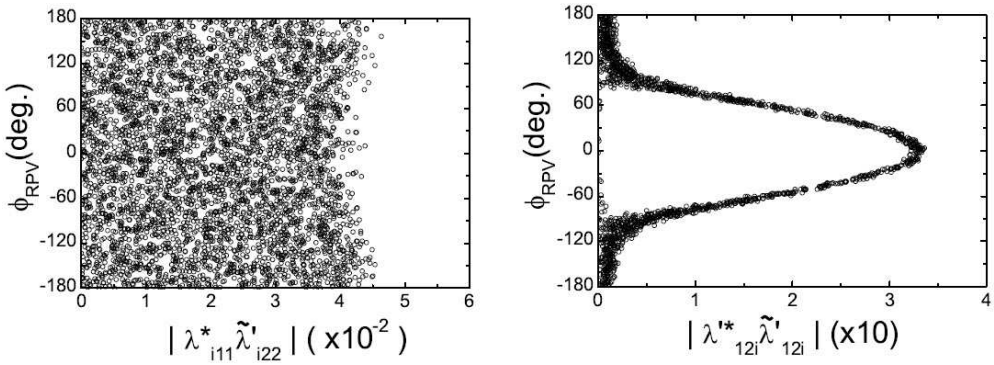

Figure 8: The allowed RPV parameter spaces from the exclusive $\bar{c} \to \bar{s}e^+\nu_e$ decays at 90% CL with 500 GeV sfermion mass.

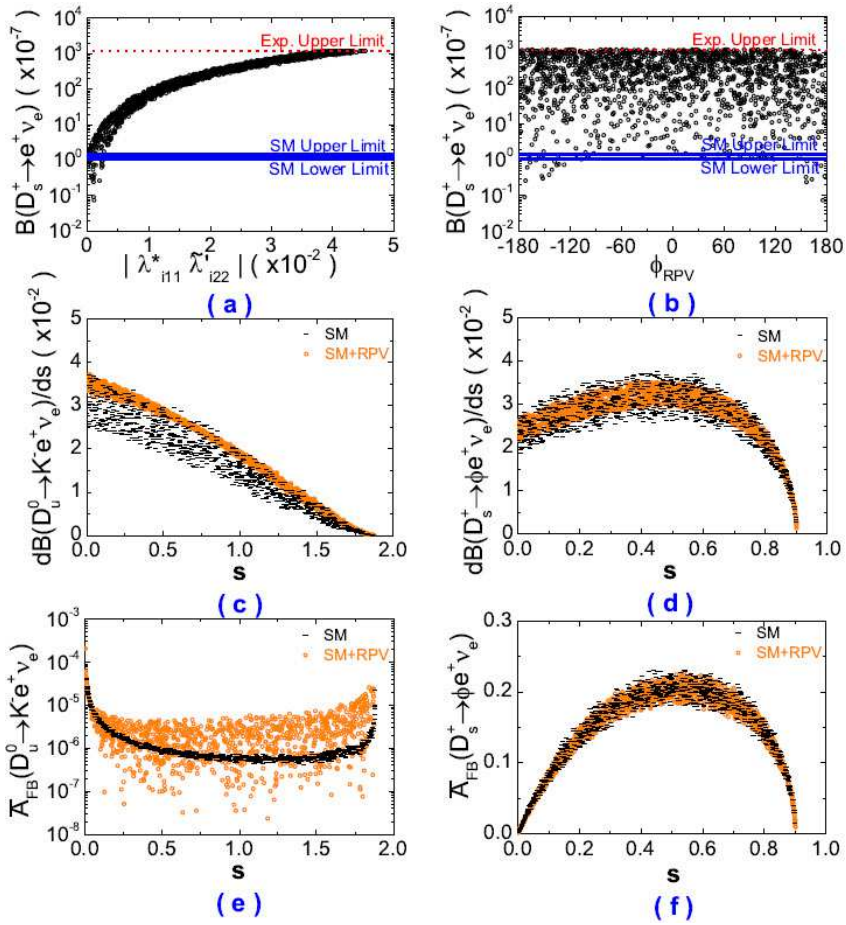

Figure 9: The constrained effects of RPV coupling $\lambda^*_{i11}\tilde{\lambda}'_{i22}$ due to the slepton exchange in the exclusive $\bar{c} \to \bar{s}e^+\nu_e$ decays.

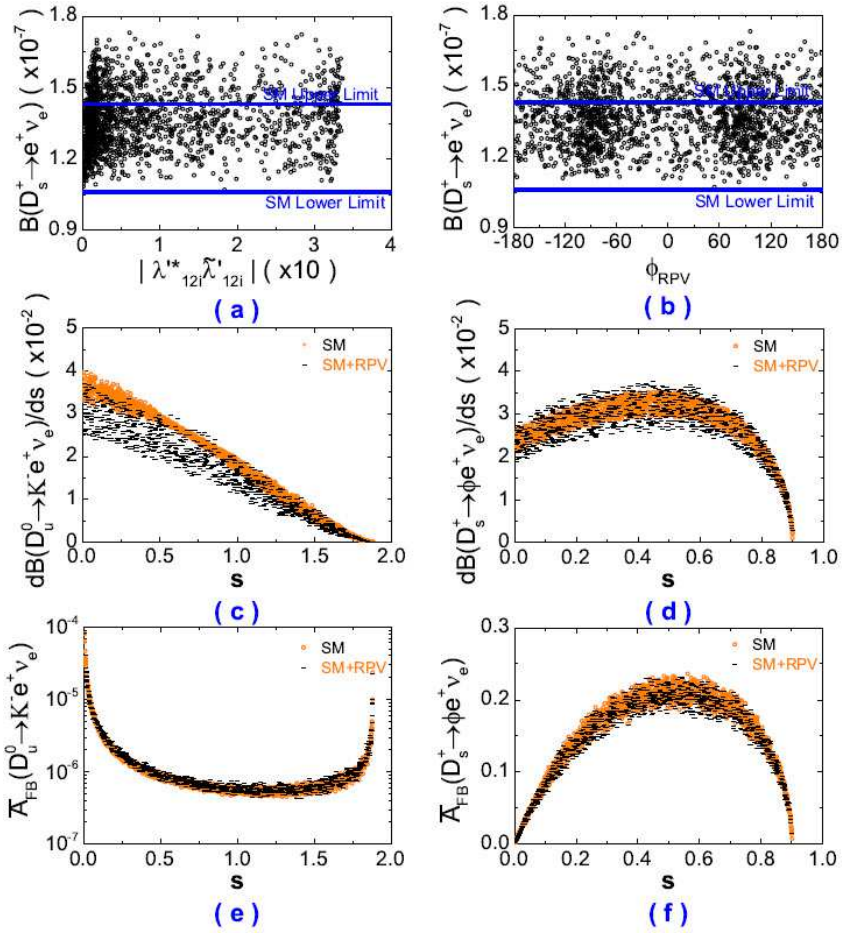

Figure 10: The constrained effects of RPV coupling $\lambda'^{*}_{12i}\tilde{\lambda}'_{12i}$ due to the squark exchange in the exclusive $\bar{c} \to \bar{s}e^{+}\nu_e$ decays.

3.4 The exclusive $\bar{c} \to \bar{s}\mu^{+}\nu_\mu$ decays

Slepton exchange coupling $\lambda^{*}_{i22}\tilde{\lambda}'_{i22}$ and squark exchange coupling $\lambda'^{*}_{22i}\tilde{\lambda}'_{22i}$ contribute to six exclusive $\bar{c} \to \bar{s}\mu^{+}\nu_\mu$ decay modes, $D_s^{+} \to \mu^{+}\nu_\mu$, $D_u^{0} \to K^{-}\mu^{+}\nu_\mu$, $D_d^{+} \to K^{0}\mu^{+}\nu_\mu$, $D_u^{0} \to K^{*-}\mu^{+}\nu_\mu$, $D_d^{+} \to K^{*0}\mu^{+}\nu_\mu$ and $D_s^{+} \to \phi\mu^{+}\nu_\mu$. All branching ratios of the exclusive $c \to s\mu^{+}\nu_\mu$ decays except $\mathcal{B}(D_s^{+} \to \phi\mu^{+}\nu_\mu)$ have been accurately measured by CLEO-c [10, 11], BESII [17], Belle [13, 14], BABAR [15] and ALEPH [22]. And their average values from PDG [44] and the SM prediction values are listed in the second and third columns of Table 4, respectively.

Our bounds for $\lambda^{*}_{i22}\tilde{\lambda}'_{i22}$ and $\lambda'^{*}_{22i}\tilde{\lambda}'_{22i}$ from the 90% CL experimental data are demonstrated in Fig. 8. We get $|\lambda^{*}_{i22}\tilde{\lambda}'_{i22}| \leq 0.60$ and $|\lambda'^{*}_{12i}\tilde{\lambda}'_{12i}| \leq 32.70$, and both bounds are derived for the first time. The constrained RPV effects in the exclusive $\bar{c} \to \bar{s}\mu^{+}\nu_\mu$ decays are also explored. The numerical results for the branching ratios are listed in the last two columns of Table 4. The constrained RPV effects

Table 4: Branching ratios of the exclusive $\bar{c} \to \bar{s}\mu^+\nu_\mu$ decays (in units of 10^{-2}) except for $\mathcal{B}(D_s^+ \to \mu^+\nu_\mu)$ (in units of 10^{-3}). "a" denotes the experimental data and "b" denotes the corresponding experimental bounds at 90% CL.

Observable	Exp. data	SM predictions	SUSY w/$\lambda^*_{i22}\tilde{\lambda}'_{i22}$	SUSY w/$\lambda'^*_{22i}\tilde{\lambda}'_{22i}$
$\mathcal{B}(D_s^+ \to \mu^+\nu_\mu)$	$(5.90\pm0.33)^a$ $[5.36,6.44]^b$	$[4.52, 6.10]$	$[5.36, 6.44]$	$[5.36, 6.44]$
$\mathcal{B}(D_u^0 \to K^-\mu^+\nu_\mu)$	$(3.31\pm0.13)^a$ $[3.10,3.52]^b$	$[2.10, 5.42]$	$[3.20, 3.52]$	$[3.21, 3.52]$
$\mathcal{B}(D_d^+ \to K^0\mu^+\nu_\mu)$	$(9.2\pm0.6)^a$ $[8.22,10.18]^b$	$[5.37, 9.94]$	$[8.22, 9.03]$	$[8.22, 9.03]$
$\mathcal{B}(D_u^0 \to K^{*-}\mu^+\nu_\mu)$	$(1.91\pm0.24)^a$ $[1.52,2.30]^b$	$[1.79, 2.32]$	$[1.96, 2.19]$	$[1.96, 2.19]$
$\mathcal{B}(D_d^+ \to K^{*0}\mu^+\nu_\mu)$	$(5.28\pm0.15)^a$ $[5.03,5.53]^b$	$[4.55, 5.91]$	$[5.03, 5.53]$	$[5.03, 5.53]$
$\mathcal{B}(D_s^+ \to \phi\mu^+\nu_\mu)$	$\cdots$	$[1.99, 2.79]$	$[2.07, 3.03]$	$[2.04, 3.42]$

due to the slepton exchange and squark exchange are displayed in Fig. 12 and Fig. 13, respectively. Noted that the RPV effects in the exclusive $\bar{c} \to \bar{s}\mu^+\nu_\mu$ decays are similar to ones in the exclusive $\bar{c} \to \bar{d}\mu^+\nu_\mu$ decays.

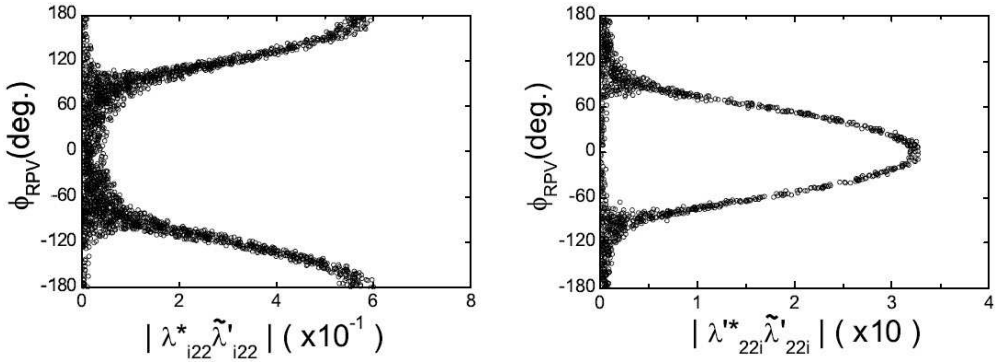

Figure 11: The allowed RPV parameter spaces from the exclusive $\bar{c} \to \bar{s}\mu^+\nu_\mu$ decays at 90% CL with 500 GeV sfermion mass.

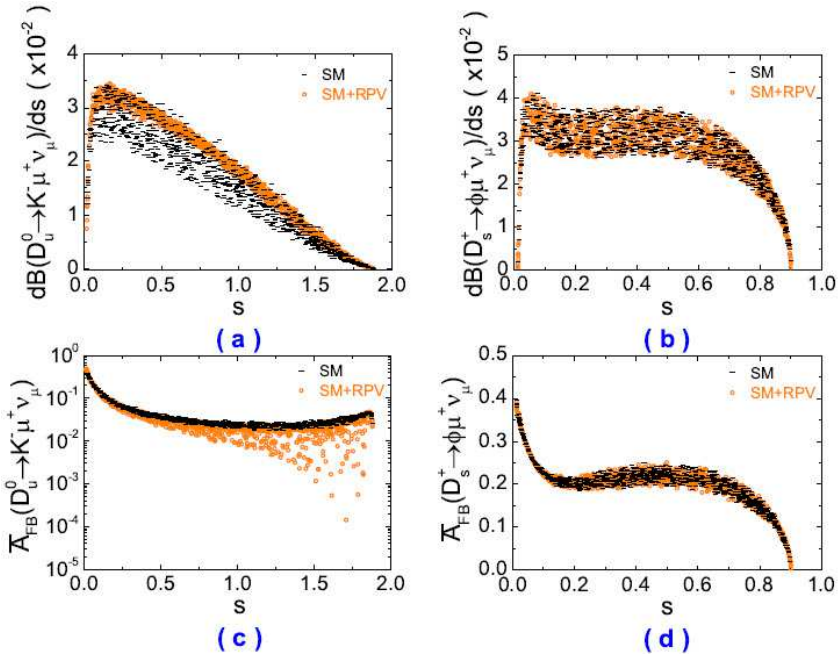

Figure 12: The constrained effects of RPV coupling $\lambda^*_{i22}\tilde{\lambda}'_{i22}$ due to the slepton exchange in the exclusive $\bar{c} \to \bar{s}\mu^+\nu_\mu$ decays.

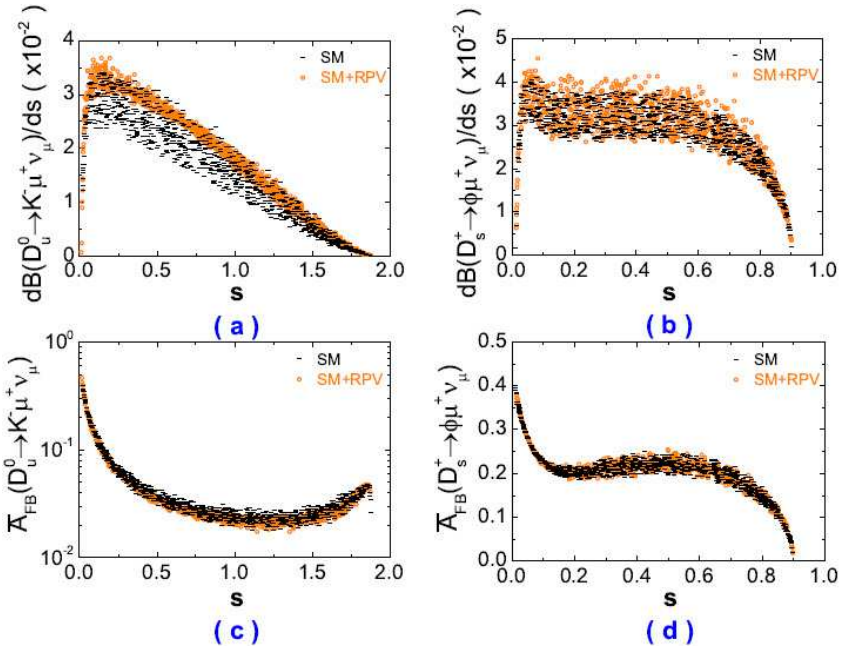

Figure 13: The constrained effects of RPV coupling $\lambda'^*_{22i}\tilde{\lambda}'_{22i}$ due to the squark exchange in the exclusive $\bar{c} \to \bar{s}\mu^+\nu_\mu$ decays.

4 Conclusion

In this paper, we have studied RPV effects in the 26 semileptonic and leptonic D meson decays, $D_d \to \ell\nu_\ell$, $D_u \to \pi\ell\nu_\ell$, $D_d \to \pi\ell\nu_\ell$, $D_s \to K\ell\nu_\ell$, $D_u \to \rho\ell\nu_\ell$, $D_d \to \rho\ell\nu_\ell$, $D_s \to K^*\ell\nu_\ell$, $D_s \to \ell\nu_\ell$, $D_u \to K\ell\nu_\ell$, $D_d \to K\ell\nu_\ell$, $D_u \to K^*\ell\nu_\ell$, $D_d \to K^*\ell\nu_\ell$ and $D_s \to \phi\ell\nu_\ell$ with $\ell = e, \mu$. Considering the theoretical uncertainties and the experimental errors, we have constrained fairly parameter spaces of RPV coupling constants from the present experimental data, and many obounds are obtained for the first time. Furthermore, we have predicted the RPV effects on the branching ratios, the differential branching ratios and the normalized FB asymmetries of charged leptons, which have not been measured or have not been well measured yet.

We have found that the constrained RPV effects due to slepton exchange could be large on the branching ratios of $D_{d/s} \to e\nu_e$ decays and the normalized FB asymmetries of $D_{u/d} \to \pi/K\ell\nu_\ell$ as well as $D_s \to K\ell\nu_\ell$ decays. The RPV contributions due to squark exchange couplings could enhance the predictions of all semileptonic branching ratios, which are very sensitive to both moduli and weak phases of the relevent RPV coupling products. Such correlated signals would provide strong evidence for RPV interactions. The results in this paper could be useful for probing the RPV SUSY effects, and will correlate strongly with searches for the direct SUSY signals at future experiments.

Acknowledgments

The work was supported by the National Natural Science Foundation of China (No. 11105115), Joint Funds of the National Natural Science Foundation of China (No. U1204113), Program for New Century Excellent Talents in University (No. NCET-12-0698), and Natural Research Project of Henan Province (No. 2011A140023).

Appendix: Input parameters

The input parameters except the form factors are collected in Table 5. In our numerical results, we will use the input parameters,which are varied randomly within 1σ range.

For the form factors involving the $D \to P(V)$ transitions, we will use the lightcone QCD sum rules ($LCSRs$) results [43]. For the $s-$dependence of the form factors, they can be parameterized in terms of simple formulae with two or three parameters. To get reasonable behavior of the form factors

Table 5: Default values of the input parameters and the 1σ error ranges for the sensitive parameters used in our numerical calculations.

$m_{K^\pm} = 0.493677 \pm 0.000016\ GeV, \quad m_{K^0} = 0.497614 \pm 0.000024\ GeV,$	
$m_{\pi^\pm} = 0.13957018 \pm 0.00000035\ GeV, \quad m_{\pi^0} = 0.1349766 \pm 0.0000006\ GeV,$	
$m_{K^{*\pm}} = 0.89166 \pm 0.00026\ GeV, \quad m_{K^{*0}} = 0.89594 \pm 0.00022\ GeV,$	
$m_{\rho^\pm} = 0.77511 \pm 0.00034\ GeV, \quad m_{\rho^0} = 0.77526 \pm 0.00025\ GeV,$	
$m_{\phi^0} = 1.019455 \pm 0.000020\ GeV, \quad \overline{m}_c(\overline{m}_c) = 1.275 \pm 0.0025\ GeV,$	
$\overline{m}_e(2GeV) = 0.0048^{+0.0005}_{-0.0003}\ GeV, \quad \overline{m}_s(2GeV) = 0.095 \pm 0.005\ GeV,$	
$m_W = 80.385 \pm 0.015\ GeV, \quad m_c = 1.67 \pm 0.07\ GeV,$	
$m_e = 0.000510998928 \pm 0.000000000011\ GeV, \quad m_\mu = 0.1056583715 \pm 0.0000000035\ GeV,$	
$m_{D_d} = 1.86962 \pm 0.00015\ GeV, \quad m_{D_s} = 1.96850 \pm 0.00032\ GeV,$	
$m_{D_u} = 1.86486 \pm 0.00013\ GeV.$	[44]
$\tau_{D_u} = 0.4101 \pm 0.0015\ ps, \quad \tau_{D_s} = 0.500 \pm 0.007\ ps, \quad \tau_{D_d} = 1.040 \pm 0.007\ ps.$	[44]
$f_{D_d} = 0.201 \pm 0.017\ GeV, \quad f_{D_s} = 0.249 \pm 0.017\ GeV.$	[46]
$\lvert V_{cd}\rvert = 0.22520 \pm 0.0065, \quad \lvert V_{cs}\rvert = 0.97344 \pm 0.00016.$	[44]

in the whole kinematically accessible region, we use the following parametrization

$$F(q^2) = \frac{F(0)}{1 - a_F q^2/m_M^2 + b_F (q^2/m_M^2)^2}, \tag{27}$$

where $F(q^2)$ can be any of the form factors $f_+, f_0, A_1, A_2, A_3^{'}$ and V. For $D \to \pi(K)$ decays, we may use the single pole approximations for the form factor f_+ in the large q^2 region [43].

$$f_+(q^2) = \frac{f_{M^*} g_{M^*} M_\pi}{2 m_{M^*}(1 - q^2/m_{M^*}^2)}, \tag{28}$$

with $f_{D^*} g_{D^*} D_\pi = 2.7 \pm 0.8 GeV, f_{D_s^*} g_{D_s^*} D_K = 3.1 \pm 0.6 GeV$. With the above considerations, we obtain the form factors in the whole kinematically accessible region shown in numerical results are presented in Table 6.

Table 6: Fit for form factors involving the $D \to \pi(K, K^*, \rho)$ and $D_s \to \phi(K, K^*)$ transitions valid for general s [43].

Decay	F(0)		a_F	b_F
$D \to \pi$	f_+	$0.635^{+0.060}_{-0.057}$	$1.01^{-0.12}_{+0.14}$	$0.17^{-0.10}_{+0.13}$
	f_0	$0.635^{+0.060}_{-0.057}$	$0.64^{-0.01}_{+0.07}$	$-0.20^{-0.04}_{+0.09}$
$D \to K$	f_+	$0.661^{+0.067}_{-0.066}$	$1.23^{-0.20}_{+0.22}$	$0.69^{-0.15}_{+0.18}$
	f_0	$0.661^{+0.067}_{-0.066}$	$0.80^{-0.03}_{+0.05}$	$-0.22^{-0.04}_{+0.06}$
$D_s \to K$	f_+	$0.820^{+0.080}_{-0.071}$	$1.11^{-0.04}_{+0.07}$	$0.49^{-0.05}_{+0.06}$
	f_0	$0.820^{+0.080}_{-0.071}$	$0.53^{-0.03}_{+0.04}$	$-0.07^{-0.04}_{+0.04}$
$D \to K^*$	A_1	$0.571^{+0.020}_{-0.022}$	$0.65^{-0.06}_{+0.10}$	$0.66^{-0.18}_{+0.21}$
	A_2	$0.345^{+0.034}_{-0.037}$	$1.86^{+0.05}_{-0.22}$	$-0.91^{+0.48}_{-0.97}$
	$A_3^{'}$	$-0.723^{+0.065}_{-0.077}$	$1.32^{+0.14}_{-0.09}$	$1.28^{+0.22}_{-0.21}$
	V	$0.791^{+0.024}_{-0.026}$	$1.04^{-0.17}_{+0.25}$	$2.21^{-0.12}_{+0.37}$
$D \to \rho$	A_1	$0.599^{+0.035}_{-0.030}$	$0.44^{-0.06}_{+0.10}$	$0.58^{-0.04}_{+0.23}$
	A_2	$0.372^{+0.026}_{-0.031}$	$1.64^{-0.16}_{+0.10}$	$0.56^{-0.28}_{+0.04}$
	$A_3^{'}$	$-0.719^{+0.055}_{-0.066}$	$1.05^{+0.15}_{-0.15}$	$1.77^{-0.11}_{+0.20}$
	V	$0.801^{+0.044}_{-0.036}$	$0.78^{-0.20}_{+0.24}$	$2.61^{+0.29}_{-0.04}$
$D_s \to K^*$	A_1	$0.589^{+0.040}_{-0.042}$	$0.56^{-0.02}_{+0.02}$	$-0.12^{+0.03}_{-0.02}$
	A_2	$0.315^{+0.024}_{-0.018}$	$0.15^{+0.22}_{-0.14}$	$0.24^{-0.94}_{+0.83}$
	$A_3^{'}$	$-0.675^{+0.027}_{-0.037}$	$0.48^{-0.11}_{+0.13}$	$-0.14^{+0.18}_{-0.17}$
	V	$0.771^{+0.049}_{-0.049}$	$1.08^{-0.02}_{+0.02}$	$0.13^{+0.03}_{-0.02}$
$D_s \to \phi$	A_1	$0.569^{+0.046}_{-0.049}$	$0.84^{-0.05}_{+0.06}$	$0.16^{-0.01}_{+0.01}$
	A_2	$0.304^{+0.021}_{-0.017}$	$0.24^{+0.18}_{-0.05}$	$1.25^{-1.08}_{+1.02}$
	$A_3^{'}$	$-0.757^{+0.029}_{-0.039}$	$0.60^{-0.02}_{+0.07}$	$0.60^{+0.31}_{-0.33}$
	V	$0.778^{+0.057}_{-0.062}$	$1.37^{-0.05}_{+0.04}$	$0.52^{+0.04}_{-0.06}$

References

[1] H. Ma, PoS Hadron **2013**, 076 (2014).

[2] H. -B. Li, Nucl. Phys. Proc. Suppl. **233**, 185 (2012) [arXiv:1209.3059 [hep-ex]].

[3] G. Huang (BESIII Collaboration), arXiv:1209.4813 [hep-ex].

[4] M. Ablikim *et al.* (BESIII Collaboration), Phys. Rev. D **89**, 051104 (2014) [arXiv:1312.0374 [hep-ex]].

[5] D. Besson *et al.* (CLEO Collaboration), Phys. Rev. D **80**, 032005 (2009) [arXiv:0906.2983 [hep-ex]].

[6] G. S. Huang *et al.* (CLEO Collaboration), Phys. Rev. Lett. **95**, 181801 (2005) [hep-ex/0506053].

[7] T. E. Coan *et al.* (CLEO Collaboration), Phys. Rev. Lett. **95**, 181802 (2005) [hep-ex/0506052].

[8] J. Yelton *et al.* (CLEO Collaboration), Phys. Rev. D **80**, 052007 (2009) [arXiv:0903.0601 [hep-ex]].

[9] B. I. Eisenstein *et al.* (CLEO Collaboration), Phys. Rev. D **78**, 052003 (2008) [arXiv:0806.2112 [hep-ex]].

[10] R. A. Briere *et al.* (CLEO Collaboration), Phys. Rev. D **81**, 112001 (2010) [arXiv:1004.1954 [hep-ex]].

[11] J. P. Alexander *et al.* (CLEO Collaboration), Phys. Rev. D **79**, 052001 (2009) [arXiv:0901.1216 [hep-ex]].

[12] K. M. Ecklund *et al.* (CLEO Collaboration), Phys. Rev. D **80**, 052009 (2009) [arXiv:0907.3201 [hep-ex]].

[13] L. Widhalm *et al.* (Belle Collaboration), Phys. Rev. Lett. **97**, 061804 (2006) [hep-ex/0604049].

[14] L. Widhalm *et al.* (Belle Collaboration), Phys. Rev. Lett. **100**, 241801 (2008) [arXiv:0709.1340 [hep-ex]].

[15] P. del Amo Sanchez *et al.* (BaBar Collaboration), Phys. Rev. D **82**, 091103 (2010) [arXiv:1008.4080 [hep-ex]].

[16] B. Aubert *et al.* (BaBar Collaboration), Phys. Rev. D **78**, 051101 (2008) [arXiv:0807.1599 [hep-ex]].

[17] M. Ablikim *et al.* (BES Collaboration), Phys. Lett. B **644**, 20 (2007) [hep-ex/0610020].

[18] M. Ablikim *et al.* (BES Collaboration), Phys. Lett. B **610**, 183 (2005) [hep-ex/0410050].

[19] M. Ablikim *et al.* (BES Collaboration), Phys. Lett. B **608**, 24 (2005) [hep-ex/0410030].

[20] M. Ablikim *et al.* (BES Collaboration), Eur. Phys. J. C **47**, 31 (2006) [hep-ex/0605103].

[21] M. Ablikim *et al.* (BES Collaboration), Phys. Lett. B **597**, 39 (2004) [hep-ex/0406028].

[22] A. Heister *et al.* (ALEPH Collaboration), Phys. Lett. B **528**, 1 (2002) [hep-ex/0201024].

[23] J. Adler *et al.* (MARK-III Collaboration), Phys. Rev. Lett. **62**, 1821 (1989).

[24] J. Barranco, D. Delepine, V. Gonzalez Macias and L. Lopez-Lozano, arXiv:1404.0454 [hep-ph].

[25] J. Barranco, D. Delepine, V. Gonzalez Macias and L. Lopez-Lozano, Phys. Lett. B **731**, 36 (2014) [arXiv:1303.3896 [hep-ph]].

[26] A. G. Akeroyd and F. Mahmoudi, JHEP **0904**, 121 (2009) [arXiv:0902.2393 [hep-ph]].

[27] B. A. Dobrescu and A. S. Kronfeld, Phys. Rev. Lett. **100**, 241802 (2008) [arXiv:0803.0512 [hep-ph]].

[28] A. G. Akeroyd and C. H. Chen, Phys. Rev. D **75**, 075004 (2007) [hep-ph/0701078].

[29] S. Fajfer and J. F. Kamenik, Phys. Rev. D **73**, 057503 (2006) [hep-ph/0601028].

[30] S. Fajfer and J. F. Kamenik, Phys. Rev. D **72**, 034029 (2005) [hep-ph/0506051].

[31] S. Fajfer and J. F. Kamenik, Phys. Rev. D **71**, 014020 (2005) [hep-ph/0412140].

[32] A. G. Akeroyd, Prog. Theor. Phys. **111**, 295 (2004) [hep-ph/0308260].

[33] A. G. Akeroyd and S. Recksiegel, Phys. Lett. B **554**, 38 (2003) [hep-ph/0210376].

[34] S. Weinberg, Phys. Rev. D **26**, 287 (1982).

[35] M. Chemtob, Prog. Part. Nucl. Phys. **54**, 71 (2005) [hep-ph/0406029].

[36] A. A. Petrov and G. K. Yeghiyan, Phys. Rev. D **77**, 034018 (2008) [arXiv:0710.4939 [hep-ph]].

[37] E. Golowich, S. Pakvasa and A. A. Petrov, Phys. Rev. Lett. **98**, 181801 (2007) [hep-ph/0610039].

[38] S. -L. Chen, X. -G. He, A. Hovhannisyan and H. -C. Tsai, JHEP **0709**, 044 (2007) [arXiv:0706.1100 [hep-ph]].

[39] S. Nandi and J. P. Saha, Phys. Rev. D **74**, 095007 (2006) [hep-ph/0608341].

[40] G. Bhattacharyya and A. Raychaudhuri, Phys. Rev. D **57**, 3837 (1998) [hep-ph/9712245].

[41] A. Kundu and J. P. Saha, Phys. Rev. D **70**, 096002 (2004) [hep-ph/0403154].

[42] B. Grinstein *et al.*, Nucl. Phys. B **380**, 369 (1992) [hep-ph/9204207].

[43] Y. -L. Wu, M. Zhong and Y. -B. Zuo, Int. J. Mod. Phys. A **21**, 6125 (2006) [hep-ph/0604007].

[44] J. Beringer *et al.* (Particle Data Group Collaboration), Phys. Rev. D **86**, 010001 (2012) and 2013 partial update for the 2014 edition.

[45] Ru-Min Wang *et al.*, in preparation.

[46] C. Aubin *et al.*, Phys. Rev. Lett. **95**, 122002 (2005) [hep-lat/0506030].